INSTITUTE OF PHYSICS PUBLISHING JOURNAL OF OPTICS A: PURE AND APPLIED OPTICS

J. Opt. A: Pure Appl. Opt. **6** (2004) 698–702 PII: S1464-4258(04)76088-2

The measurement and modelling of light scattering by phytoplankton cells at narrow forward angles

Iain MacCallum[1], **Alex Cunningham**[2] **and David McKee**

Physics Department, University of Strathclyde, 107 Rottenrow, Glasgow G4 ONG, UK

E-mail: a.cunningham@strath.ac.uk

Received 10 February 2004, accepted for publication 29 March 2004
Published 11 June 2004
Online at stacks.iop.org/JOptA/6/698
doi:10.1088/1464-4258/6/7/007

Abstract
A procedure has been devised for measuring the angular dependence of light scattering from suspensions of phytoplankton cells at forward angles from 0.25° to 8°. The cells were illuminated with a spatially-filtered laser beam and the angular distribution of scattered light measured by tracking a photodetector across the Fourier plane of a collecting lens using a stepper-motor driven stage. The procedure was calibrated by measuring scattering from latex bead suspensions with known size distributions. It was then used to examine the scattering from cultures of the unicellular algae *Isochrysis galbana* (4 μm × 5 μm), *Dunaliella primolecta* (6 μm × 7 μm) and *Rhinomonas reticulata* (5 μm × 11 μm). The results were compared with the predictions of Mie theory. Excellent agreement was obtained for spherical particles. A suitable choice of spherical-equivalent scattering parameters was required to enable reasonable agreement within the first diffraction lobe for ellipsoidal particles.

Keywords: diffraction and scattering, Fourier optics, optical properties of seawater

1. Introduction

Phytoplankton cells play a major part in determining variations in the optical properties of natural waters. Since these cells are typically much larger than visible wavelengths, they scatter light predominantly at narrow forward angles [1, 2]. This has important practical consequences for underwater optics. Forward scattering plays a major role in determining the point spread function, which quantifies the degradation of an image viewed through a scattering medium [3–6]. It is a limiting factor in the performance of oceanographic transmissometers, which should be designed to reject scattered light [7]. It is employed in instruments for measuring the size distribution of marine suspensions [8, 9] and is measured directly in flow cytometers, which are increasingly being used to analyse natural phytoplankton populations [10, 11]. Although several studies of the angular distribution of phytoplankton scattering have been carried out, little information is available on scattering at narrow forward angles. This is partly due to the problem of discriminating the scattered light from the illuminating beam, and partly to the strong dependence of the sensing volume on viewing angle when swinging-arm detectors are employed [12, 13]. In this paper, we report the construction of an instrument that measures scattering in the range of 0.25°–8° by recording variations of intensity in the Fourier plane of a collecting lens. An earlier attempt using this approach was hampered by limitations in the available technology, and provided measurements only at sub-degree angles [14]. The performance of the new instrument was validated using latex calibration beads, and it was then used to evaluate Mie-theory predictions of scattering from phytoplankton suspensions. In the first instance, we consider species that are ellipsoidal in shape with significantly different mean cell sizes.

[1] Present address: College of Oceanic and Atmospheric Sciences, Oregon State University, Corvallis, OR 97331-5503, USA.
[2] Author to whom any correspondence should be addressed.

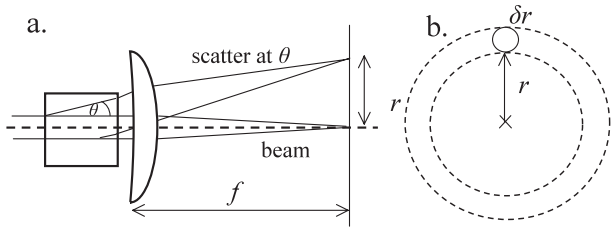

Figure 1. Optical principles of near-forward scattering measurements in the Fourier plane of a collecting lens.

2. Methodology

2.1. Theory

When a converging lens of focal length f collects light scattered from a collimated beam, the distribution of intensity in the focal plane represents an optical Fourier transform in which the radial distance from the axis r is related to the scattering angle θ by $r = f \tan\theta$ [15]. The undeviated portion of the illuminating beam is concentrated at the focal point, and this makes it relatively easy to distinguish between directly transmitted and scattered light at sub-degree angles. In order to relate the signal recorded by a small-area detector to the angular distribution of scattering from a sample in suspension, it is necessary to consider the geometry of the apparatus (figure 1). Light scattered at an angle θ_w in water of refractive index n_w leaves the cuvette at an angle θ_a in air, where $\sin\theta_a = n_w \sin\theta_w$. The corresponding solid angle is $\omega_a = 4\pi \sin^2\theta_a$. A pinhole of radius d$r$ positioned in the focal plane of a lens samples a fraction F of the light leaving the cuvette in an element of solid angle (dω_a), which is represented in the focal plane of the lens by an annulus with the radial limits (r + dr). The sampling efficiency F is determined by the ratio of the area of the pinhole to that of the annulus, and depends on the angle of the inner edge of the pinhole relative to the optical axis (θ_a) according to

$$F = \frac{(\mathrm{d}r)^2}{(\mathrm{d}r)^2 + 2f(\tan\theta_a)(\mathrm{d}r)}.$$

For the work described here, no attempt was made to measure absolute scattering intensities. Instead, the angular pattern was expressed as a fraction of the signal recorded at the smallest scattering angle that could be measured (approximately 0.25°).

2.2. Instrumentation

Light from a 10 mW helium neon laser (632.8 nm) was passed through a spatial filter and beam expander to generate an illuminating beam with a diameter of 4 mm and divergence of 0.1 mrad. The intensity of the expanded beam was monitored using a beam splitter and reference photodiode, and a series of apertures were placed in the beam path to remove non-collimated scattering and reflection from optical components. The particle suspension was held in a rectangular glass cuvette (Helma, Germany) with polished walls and a 10 mm path length. A plano-convex lens of 25 mm diameter and 200 mm focal length, positioned close to the cuvette wall, collected light that passed through the cuvette. This lens brought the illuminating beam to a focus of approximately 200 μm diameter ($1/e^2$ points) and collected all light scattered by particles in the cuvette at angles up to 15° (in water). The scattered light detector consisted of a large-area (41 mm^2) silicon photodiode mounted 1 mm behind a 0.6 mm diameter pinhole so that all the light entering the pinhole was collected by the diode. The current from the photodiode was converted to a voltage using an FET-input amplifier and digitized using a National Instruments 12-bit AD card with a programmable gain stage. Detectable signals ranged from a maximum of 10 V to a noise level of around 5 mV. The scattering detector was mounted on a carrier and moved across the Fourier plane of the collecting lens by a lead screw driven by a stepper motor. The detector was advanced in steps corresponding to 0.034° increments in scattering angle, and the signal averaged by acquiring sequential samples over a 200 ms period at each step. A desktop computer was used to control the stepper motor and the AD card, and the duration of a typical scan was approximately 5 min. The linearity of the detector was checked using a series of neutral density filters, and the angular accuracy of the equipment established by placing a series of pinholes of known diameter in the beam and monitoring the resulting diffraction patterns. For repeated scans of a single diffraction pattern, the mean standard deviation of the measurements over angles from 0° to 10° was 2.3%.

Table 1. The physical properties of phytoplankton cells. Mean values of the major and minor axes of approximate ellipsoids (d_1 and d_2) were measured by microscopy for 1000 cells. The mean radii (a) and population standard deviation (σ) were then calculated for spheres of equivalent volume. The alternative values for σ, in parentheses, are those that produced the best fit to the measured curves. The real and imaginary components of the refractive index in water (n_r and n_i) were derived from anomalous diffraction theory. All sizes are measured in micrometres.

			Measured			
Species	d_1	d_2	a	σ	n_r	n_i
Isochrysis galbana	5	4.1	2.2	0.09 (0.14)	1.04	0.0012
Dunaliella primolecta	7	5.9	3.2	0.12 (0.18)	1.03	0.0018
Rhinomonas reticulata	10.5	4.8	3.2	0.09 (0.2)	1.03	0.0015

2.3. Calibration beads and phytoplankton cells

The instrument correction procedure was checked using polystyrene latex microbeads (Dyno Particles, Norway). These beads had certified size distributions, with means and standard deviations of 5 ± 0.31 and 15 ± 0.55 μm. The real component of their refractive index relative to water was 1.19 at 632 nm, and the imaginary component was taken to be zero. The phytoplankton species chosen were *Isochrysis galbana*, *Dunaliella primolecta*, and *Rhinomonas reticulata*. The cultures were maintained in an enriched seawater medium in an incubator at 18 °C under continuous illumination. These species are all single-celled flagellates with an approximately ellipsoidal shape whose longest dimension varied from 5 μm (*Isochrysis*) to 10.5 μm (*Rhinomonas*). The lengths of the major and minor axes of 1000 individuals of each species were measured by video optical microscopy, and the apparent

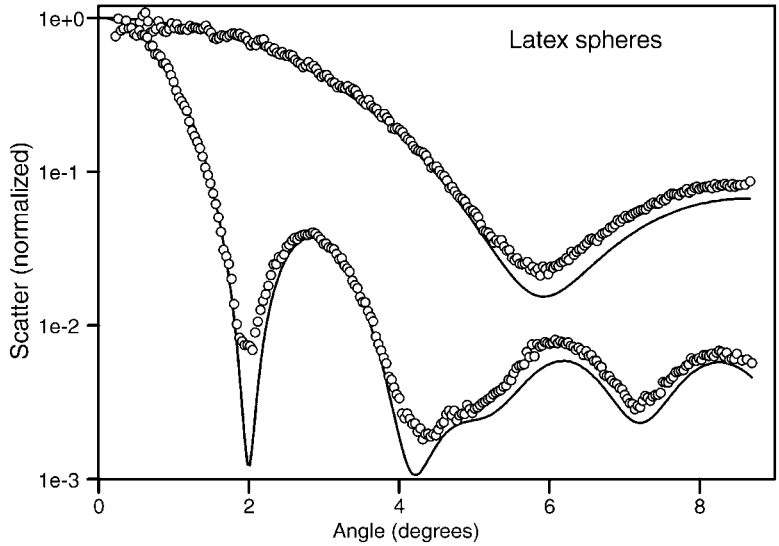

Figure 2. Near forward-angle scattering from suspensions of latex beads of mean diameter 5 and 15 μm, with results calculated by Mie theory superimposed.

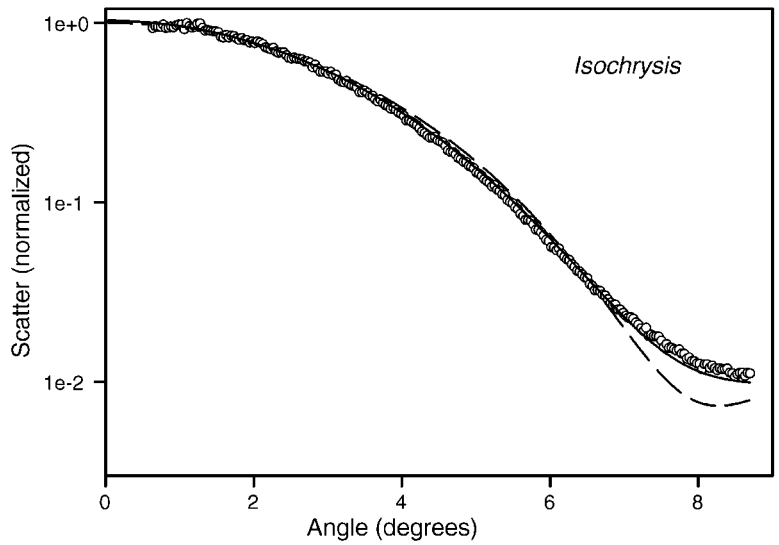

Figure 3. Scattering from a suspension of *Isochrysis galbana* (approximate size 5 μm $\times$ 4 μm). Measurements are indicated with open circles. Results from Mie theory are shown for the equivalent sphere parameters measured by video microscopy (broken curve) and with an increased value for the standard deviation of the size parameter (solid curve: see table 1).

refractive index of the cells was derived by the procedure described in Stramski *et al* [16]. This procedure involves measuring the average absorption and scattering cross sections of cells in suspension and inverting the data using anomalous diffraction theory. The results are summarized in table 1.

2.4. Measurement procedure

A first scan of the light pattern in the plane of the detector was made with 0.2 μm filtered growth medium in the cuvette in order to determine the profile of the focused laser beam, which was several orders of magnitude more intense than the scattering signals. A second scan was then carried out after a small volume of the latex bead suspension or concentrated phytoplankton culture had been added. Care was taken to avoid disturbing the position of the cuvette when the sample was added. The angular distribution of the light scattered by the sample was obtained by subtracting the signals from the two scans. In practice the scattering signal could be distinguished from the laser beam at minimum angles ranging from 0.25° to 0.4°, depending on the alignment of the optics in a given run. In order to minimize the effect of multiple scattering, it was necessary to keep the optical thickness of the suspension below 0.3 [1].

2.5. Mie calculations

Mie calculations were carried out using code written in our laboratory and validated against the results of published scattering calculations [17]. In order to carry out Mie calculations it is necessary to specify the illuminating wavelength, the particle size distribution in terms of mean diameter and standard deviation, and the refractive index of the particles relative to the suspending medium. The result is

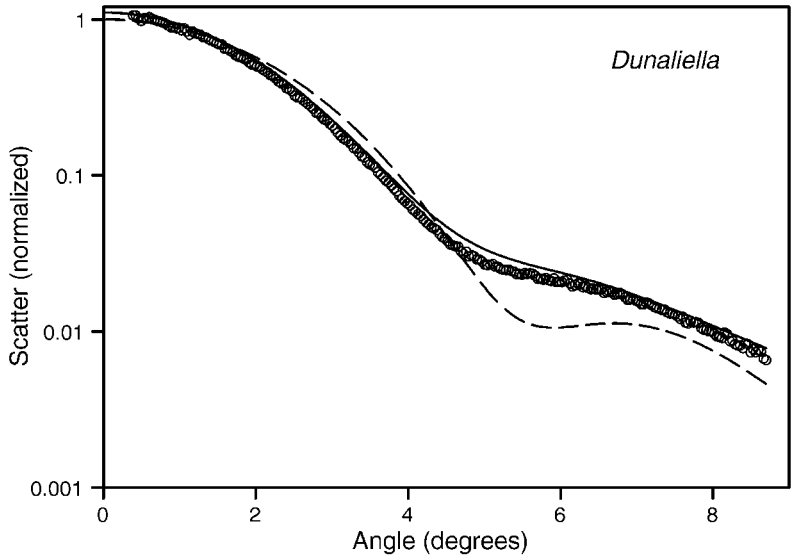

Figure 4. Scattering curves for *Dunaliella primolecta* (approximate size 7 μm $\times$ 6 μm) with details as for figure 3.

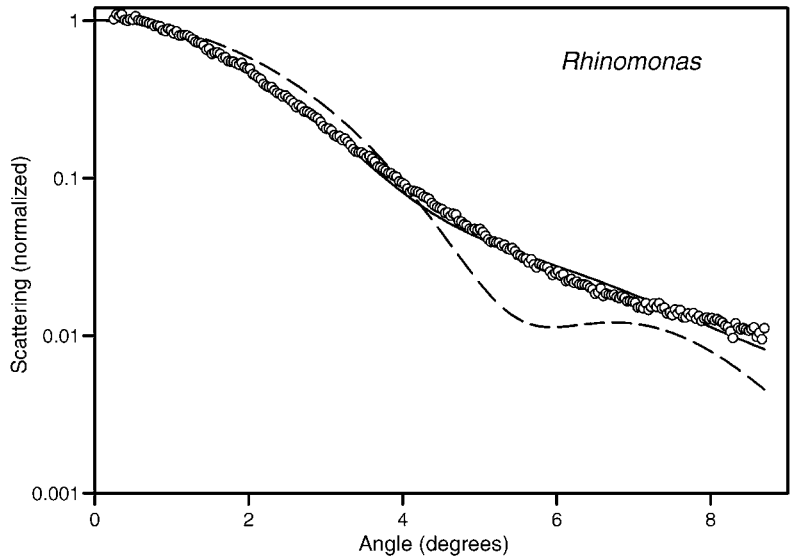

Figure 5. Scattering curves for *Rhodomonas reticulata* (approximate size 11 μm $\times$ 5 μm) with details as for figure 3.

usually given in terms of the scattering phase function, which specifies the relative distribution of scattered light intensity as a function of solid angle and has an integral value of unity [18]. The calculated scattering functions were normalized at 0.25° to facilitate comparison with those measured experimentally.

3. Results

3.1. Latex beads

Figure 2 shows scattering patterns measured for two sizes of latex spheres, with mean diameters of 5 and 15 μm, together with the scattering pattern calculated by Mie theory. These samples had narrow size distributions, and clearly defined maxima and minima were observed. The shape of the first scattering lobe was well matched for both particle sizes, and the angular positions of the minima accurately predicted. However, measured values of the scaled scattering functions were significantly higher than predicted values at angles beyond the first scattering lobe. This discrepancy could not be attributed to electrical noise, and may have been due to the presence of very small scattering particles in the sample, or to an increase in the polydispersity of the bead suspensions during storage and sample preparation.

3.2. Phytoplankton cells

Scattering patterns for three algal species are shown in figures 3–5. The lines drawn on each graph represent the results of two Mie calculations. One employed the equivalent-sphere parameters derived by direct measurement for each species, while the second allowed the standard deviation of the size distribution to vary until the match between theory and observation was optimized (table 1). In all cases, better fits were obtained using standard deviations for the equivalent sphere radius that were considerable greater than those directly

measured. The increase required was 61% for *Isochrysis*, 58% for *Dunaliella* and 133% for *Rhinomonas*. The most likely explanation is that the dimensions measured by microscopy were all obtained for cells aligned with their long axis perpendicular to the viewing direction, while the scattering measurements were made on cells at random orientations in suspension. The range of cross sections presented to the laser beam is clearly greater for the suspended cells. The root mean square discrepancy between the values predicted by the best-fit Mie calculation and those measured in the first 8° was below 10% for all three phytoplankton species.

4. Discussion

The chief advantages of the Fourier lens approach are the mechanical simplicity of the instrumentation and the ability to make measurements with fine angular resolution in the direction where the highest scattering intensities are produced by phytoplankton cells. The disadvantage is the limited angular range of the measurements, which in practice is around 10°. It is difficult to justify extrapolation of the scattering function to wider angles where the fine details of particle morphology can have a significant influence. The technique has been shown to work well for spheres and ellipsoidal cells, and the match between measurements and Mie theory is remarkably good if the adjustment of the size distribution parameter is accepted. The scattering phase functions that are most commonly used in modelling radiance transfer in seawater are based on the assumption that phase functions averaged over all particle types can be approximated by Mie theory [19, 20]. However, the composition of marine particle suspensions can be entirely dominated by phytoplankton cells during periods of intense growth such as the spring bloom at temperate latitudes. Many phytoplankton cells have complex shapes and exhibit strong azimuthal inhomogeneity in their single-cell scattering patterns [21]. It is therefore important to assess the degree to which Mie theory can be applied to randomly oriented cells of more complex morphology and to evaluate results from more complex optical models such as the discrete dipole approximation and T-matrix theory [22].

References

[1] van de Hulst H C 1981 *Light Scattering by Small Particles* (New York: Dover)

[2] Morel A 1994 Optics from the single cell to the mesoscale *Ocean Optics* ed R W Spinrad, K L Carder and M J Perry (New York: Oxford University Press) pp 93–106

[3] Gordon H R 1993 The sensitivity of radiative transfer to small-angle scattering in the ocean: a quantitative assessment *Appl. Opt.* **32** 7505–11

[4] Gordon H R 1994 Equivalence of the point and beam spread functions of scattering media: a formal demonstration *Appl. Opt.* **33** 1120–2

[5] Swanson N L, Billard B D, Gehman V M and Gennaro T L 2001 Application of the small-angle approximation to ocean water types *Appl. Opt.* **40** 3608–13

[6] Jaffe J S, Moore K D, McLean J and Strand M P 2001 Underwater optical imaging: status and prospects *Oceanography* **14** 66–76

[7] Bartz R, Zaneveld J R V and Pak H 1978 A transmissometer for profiling and moored observations in water *Ocean Optics V; Proc. SPIE* **160** 102–8

[8] Gartner J W, Cheng R T, Wang P F and Richter K 2001 Laboratory and field evaluations of the LISST-100 instrument for suspended particle size distributions *Marine Geol.* **175** 199–219

[9] Mikkelsen O A and Pejrup M 2001 The use of a LISST-100 laser particle sizer for *in situ* estimates of floc size, density and settling velocity *Geo-Mar. Lett.* **20** 187–95

[10] Reckermann M and Colijn F 2000 Aquatic flow cytometry: achievements and prospects *Sci. Mar.* **64** (2) 152 (Special issue)

[11] Green R E, Sosik H M and Olson R J 2003 Contributions of phytoplankton and other particles to inherent optical properties in New England continental shelf waters *Limnol. Oceanogr.* **48** 2377–91

[12] Petzold T J 1977 Volume scattering functions for selected ocean waters *Light in the Sea* ed J E Tyler (Stroudsberg: Dowden, Hutchinson and Ross) pp 150–74

[13] Volten H, de Haan J F, Hovenier J W, Schreurs R, Vassen W, Dekker A G, Hoogenboom H J, Charlton F and Wouts R 1998 Laboratory measurements of angular distributions of light scattered by phytoplankton and silt *Limnol. Oceanogr.* **43** 1180–97

[14] Spinrad R W, Zaneveld J R V and Pak H 1978 Volume scattering function of suspended particulate matter at near-forward angles: a comparison of experimental and theoretical values *Appl. Opt.* **17** 1125–30

[15] Goodman J W 1996 *Introduction to Fourier Optics* (New York: McGraw-Hill) p 441

[16] Stramski D A, Morel A and Bricaud A 1988 Modelling the light attenuation and scattering by spherical phytoplankton cells: a retrieval of the bulk refractive index *Appl. Opt.* **27** 3954–6

[17] Bohren C F and Huffman D R 1983 *Absorption and Scattering of Light by Small Particles* (New York: Wiley)

[18] Mobley C D 1994 *Light and Water: Radiative Transfer in Natural Waters* (San Diego, CA: Academic)

[19] Fournier G R and Forand J L 1994 Analytic phase function for ocean water *Ocean Optics XII; Proc. SPIE* **2258** 194–201

[20] Twardowski M S, Boss E, MacDonald J B, Pegau W S, Barnard A H and Zaneveld J R 2001 A model for estimating bulk refractive index from the optical backscattering ratio and the implications for understanding particle composition in case I and case II waters *J. Geophys. Res.* **106** 14129–42

[21] Buonaccorsi G A B and Cunningham A 1990 Azimuthal inhomogeneity in the forward light scattered from algal colonies *Limnol. Oceanogr.* **35** 1166–71

[22] Gordon H R and Du T 2001 Light scattering by nonspherical particles: application to coccoliths detached from Emiliania huxleyi *Limnol. Oceanogr.* **46** 1438–54